



HAL
open science

Biogeography of N₂ Fixation Influenced by the Western Boundary Current Intrusion in the South China Sea

Yangyang Lu, Zuozhu Wen, Dalin Shi, Wenfang Lin, Sophie Bonnet, Minhan Dai, Shuh-ji Kao

► **To cite this version:**

Yangyang Lu, Zuozhu Wen, Dalin Shi, Wenfang Lin, Sophie Bonnet, et al.. Biogeography of N₂ Fixation Influenced by the Western Boundary Current Intrusion in the South China Sea. *Journal of Geophysical Research. Oceans*, 2019, 124 (10), pp.6983-6996. 10.1029/2018JC014781 . hal-02461797

HAL Id: hal-02461797

<https://amu.hal.science/hal-02461797>

Submitted on 30 Jan 2020

HAL is a multi-disciplinary open access archive for the deposit and dissemination of scientific research documents, whether they are published or not. The documents may come from teaching and research institutions in France or abroad, or from public or private research centers.

L'archive ouverte pluridisciplinaire **HAL**, est destinée au dépôt et à la diffusion de documents scientifiques de niveau recherche, publiés ou non, émanant des établissements d'enseignement et de recherche français ou étrangers, des laboratoires publics ou privés.

Biogeography of N₂ Fixation Influenced by the Western Boundary Current Intrusion in the South China Sea

Yangyang Lu^{1,2,3}, Zuozhu Wen^{1,4}, Dalin Shi^{1,4}, Wenfang Lin^{1,4}, Sophie Bonnet⁵,
Minhan Dai^{1,3}, and Shuh Ji Kao^{1,3}

¹State Key Laboratory of Marine Environmental Science, Xiamen University, Xiamen, China, ²Key Laboratory of Marine Ecosystem and Biogeochemistry, State Oceanic Administration & Second Institute of Oceanography, Ministry of Natural Resources, Hangzhou, China, ³College of Ocean and Earth Sciences, Xiamen University, Xiamen, China, ⁴College of the Environment and Ecology, Xiamen University, Xiamen, China, ⁵Aix Marseille Université, CNRS/INSU, Université de Toulon, IRD, Mediterranean Institute of Oceanography (MIO), Marseille, France

Abstract The N₂ fixation and primary production rates were measured simultaneously using ¹⁵N₂ and ¹³C incubation assays in the northern South China Sea influenced by the Kuroshio intrusion (KI) seasonally. The degree of KI (KI index, range from 0 to 1) was assessed by applying an isopycnal mixing model. The water column integrated N₂ fixation and primary production for stations with KI index larger than 0.5 were $463 \pm 260 \mu\text{mol N}\cdot\text{m}^{-2}\cdot\text{day}^{-1}$ and $62 \pm 19 \text{mmol C}\cdot\text{m}^{-2}\cdot\text{day}^{-1}$, respectively, significantly higher than those for stations with KI index lower than 0.5 ($50 \pm 10 \mu\text{mol N}\cdot\text{m}^{-2}\cdot\text{day}^{-1}$ and $28 \pm 10 \text{mmol C}\cdot\text{m}^{-2}\cdot\text{day}^{-1}$, respectively). *Trichodesmium* was the dominant diazotroph at stations with KI index larger than 0.5, with 2 orders of magnitude higher *nifH* gene abundance than that at stations with KI index lower than 0.5. However, the highest N₂ fixation rates were found in waters with moderate KI index around 0.6, suggesting that frontal zone mixing might stimulate N₂ fixation. Our results demonstrated that diazotrophs (mainly *Trichodesmium*) were tightly associated with the KI, which modulated the biogeographic distribution of N₂ fixers. In summary, we found the transportation of *Trichodesmium* by KI, then, we quantified the fraction of KI and N₂ fixation rates in the northern South China Sea. The results suggested that KI generated a new biogeographic regime which could significantly influence the carbon and nitrogen cycles far away from the main stream.

1. Introduction

Biological productivity in the low-latitude oligotrophic ocean is largely limited by bioavailable nitrogen (Moore et al., 2013). In these systems, the nitrate supply from subsurface water is impeded by the permanent thermocline. Thus, N₂-fixing organisms (or diazotrophs) that convert inert N₂ gas into bioavailable N sustain the major part of new primary production (Capone et al., 2005).

Trichodesmium is a major diazotrophic cyanobacterium that is widespread in tropical and subtropical oceans (Capone et al., 2005). Annually, around half of the new bioavailable nitrogen introduced by N₂ fixation could be attributable to *Trichodesmium* in the global oceans (Bergman et al., 2013). Previous studies demonstrated that physical processes, such as eddies and currents, might play a vital role in shaping the spatial pattern of *Trichodesmium* in the ocean (Davis & McGillicuddy, 2006; Fong et al., 2008; Lipschultz & Owens, 1996; Olson et al., 2015; Taboada et al., 2010). In the Northern Hemisphere, elevated *Trichodesmium* abundance is often observed within anticyclone eddies (warm eddy) due to nitrogen limitation but sufficient phosphorus and iron (Davis & McGillicuddy, 2006; Fong et al., 2008; Olson et al., 2015). In addition, due to the buoyant character of *Trichodesmium* (Walsby, 1978 and Walsby et al., 1992), the ocean currents are found to spread *Trichodesmium* widely (Lipschultz & Owens, 1996; Taboada et al., 2010). However, whether the transported *Trichodesmium* is active and capable of N₂ fixation after the long-distance transportation remains unclear (Lipschultz & Owens, 1996). Moreover, the quantitative field information on how and to what extent the ocean currents may impact *Trichodesmium*-derived N₂ fixation and its association with primary production is still insufficient. Recently, several *Trichodesmium* N₂ fixation hot spots were discovered around islands, sometimes forming extensive blooms, likely due to iron supply (Berthelot et al., 2017; Bonnet et al., 2017; Dupouy et al., 2011; Shiozaki, Kodama, et al., 2014). If most of the hot spots signals could be transported to remote oceans (Shiozaki et al., 2013), it will reshape the global N₂ fixation flux and thus influence the oceanic nitrogen and carbon cycling significantly.

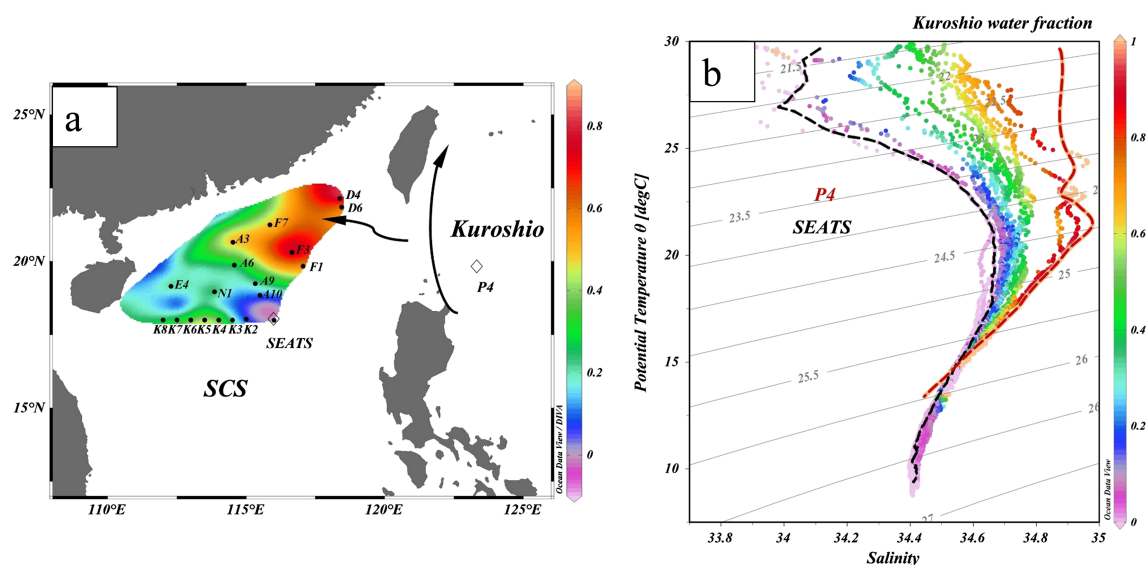


Figure 1. (a) The spatial pattern of the KI index. The color bar represents the value of $R_{\text{kave-100}}$. Black solid dots represent the sampling stations. The two open diamonds are the two end member stations (SEATS for the SCS and P4 for the Kuroshio) chosen for the isopycnal mixing model. (b) θ - S diagram of the upper 400 m for all the investigated stations. The red dashed curve denotes typical Kuroshio water, and the black dashed curve denotes typical SCS water. KI = Kuroshio intrusion; SCS = South China Sea.

The South China Sea (SCS), the largest marginal sea in the North Pacific, has a low N_2 fixation rate and *Trichodesmium* abundance during the warm season (Lee Chen et al., 2003, 2014). The reported N_2 fixation rates (with an average of $51.7 \pm 6.2 \mu\text{mol N}\cdot\text{m}^{-2}\cdot\text{day}^{-1}$) fall within the lowest range of rates ($1\text{--}100 \mu\text{mol N}\cdot\text{m}^{-2}\cdot\text{day}^{-1}$) in the global N_2 fixation database compiled by Luo et al. (2012). Such low rates and low *Trichodesmium* abundances have been attributed to a deficiency of iron and the relatively shallower nitracline in the SCS (Lee Chen et al., 2008; Wu et al., 2003). In contrast, the Kuroshio, a western boundary current to the east of the SCS, is characterized by high N_2 fixation rates ($\sim 200 \mu\text{mol N}\cdot\text{m}^{-2}\cdot\text{day}^{-1}$) mainly driven by *Trichodesmium* (Lee Chen et al., 2008, 2014). The Kuroshio intrudes into the SCS through the Luzon Strait seasonally. A previous study showed that the intrusion of nutrient-depleted Kuroshio may act as a diluter to diminish the nutrient stock in the upper water column of the SCS (Du et al., 2013). Meanwhile, the oligotrophic Kuroshio Current brings in dissolved organic carbon-enriched seawater (Wu et al., 2015), which may stimulate nitrification in the frontal zone during mixing (Xu et al., 2018). Presumably, the Kuroshio intrusion also exhibits a distinguished high *Trichodesmium* abundance and N_2 fixation rate in the SCS. This seasonal intrusion phenomenon facilitates a perfect case to investigate how the current could affect the spatial distribution and activity of *Trichodesmium* and consequently primary production in the euphotic zone in the SCS. Despite its potential significance, such an effect has not yet been explored in Pacific marginal seas. In this paper, we provide a biogeochemical view of the intrusion of a western boundary current into a marginal sea, to advance our knowledge of the coupling of carbon and nitrogen cycling in the euphotic zone of a semiclosed basin.

2. Materials and Methods

2.1. Hydrography and Nutrients

This study was conducted on board the R/V *Dongfanghong 2* in the northern South China Sea (NSCS) from 15 May to 7 July 2016. In order to investigate the potential influence of KI to N_2 fixation, 19 stations were selected from the region close to Luzon Strait to the further west region in the NSCS basin (Figure 1a). At each station, temperature and salinity were recorded by a Seabird 911 CTD. Five to six depths (corresponding to 92%, 54%, 28%, 14.4%, 8.8%, and 1% of the surface irradiance measured in our incubators) were sampled from the upper 100 m for the determination of chlorophyll a, nutrients, and *nifH* gene abundance and for

N₂ fixation and primary production incubations. Unfortunately, the photosynthetically active radiation detector was malfunctioned during our cruise. The sampling depths corresponding to each irradiance were decided using the average photosynthetically active radiation value measured previously in the NSCS during the same season (supporting information Figure S1).

Standard colorimetric techniques were used for the determination of NO₃⁻ + NO₂⁻ (NO_x) and soluble reactive phosphorus (SRP) concentrations on board with the same detection limits of 0.03 μmolL⁻¹ (Du et al., 2013). Trapezoidal integration method was used to calculate the 100 m depth-integrated nutrient concentration. The mixed layer depth (MLD) and nitracline was applied to compare the physical setting among the different stations. The MLD was defined as the depth with a 0.8 °C change from the sea surface temperature (Kara et al., 2000). The nitracline was defined as the depth at which NO_x concentration equaled 0.1 μmolL⁻¹ (Borgen et al., 2002).

2.2. Calculation of the Degree of KI Influence

To evaluate the influence of KI in the NSCS, an isopycnal mixing model proposed by Du et al. (2013) was applied. The basic assumption of this model is that isopycnal mixing dominates the mixing of water masses, which is detailed in both Du et al. (2013) and Xu et al. (2018). Two end-members are required for index estimation. Here we selected the SEATS station at 116°E/18°N to represent the proper SCS water mass end-member and P4 station at 122.959°E/20.003°N for the Kuroshio water mass end-member (Figure 1a). According to the assumption, we can quantify the proportion of the SCS (R_S) and the Kuroshio (R_K) water for any observed water parcel in the θ - S diagram in Figure 1b, basing on the conservation of either potential temperature (θ) or salinity (S) along an isopycnal surface (Figure 1b):

$$R_K + R_S = 1, \quad (1)$$

$$R_K \times \theta_K + R_S \times \theta_S = \theta \text{ or } R_K \times S_K + R_S \times S_S = S. \quad (2)$$

Note that the fraction of water mass derived from this model represents a relative value of the two selected ends instead of the absolute fraction of typical Kuroshio water since the two end-members might vary in different seasons. The average of R_K values of the upper 100 m ($R_{kave-100}$, 1 m interval) was therefore applied as a proxy, that is, the KI index to reflect the degree of KI influence at the sampling stations. The stations with KI index >0.5 were classified as KI affected, and the others were identified as the NSCS region.

2.3. N₂ Fixation and Primary Production Rate Measurements

Duplicated N₂ fixation rates were determined by the ¹⁵N₂ gas dissolved method (Mohr et al., 2010). The ¹⁵N₂ predissolved seawater was made with ¹⁵N₂ gas (98.9 atom%, Cambridge Isotope Laboratories), and a detailed procedure and the ¹⁵N₂ gas contamination tests are described in Lu et al. (2018). After preparation, 200 mL of ¹⁵N₂-enriched seawater was slowly injected into each 4.5-L polycarbonate bottle, with the enriched water constituting <5% of the total sample volume. A NaH¹³CO₃ (99 atom% ¹³C, Cambridge Isotope Laboratories) solution was added (final concentration of 100 μM) to the same bottle to measure primary production rate simultaneously. After addition of tracers, the bottle was shaken intensively before incubation.

The light conditions of the incubators were manipulated by neutral density and blue (061 Mist blue; 172 Lagoon blue) filters on deck (Mourino-Carballido et al., 2011; Rijkenberg et al., 2011). After 24 hr of incubation, precombusted GF/F filters were used to collect the particle samples (<200 mm Hg). Particulate organic matter were collected from each depth at all stations to determine background ¹⁵N-PON and ¹³C-POC natural abundance. All filter samples were stored at -20 °C immediately.

An elemental analyzer coupled to a mass spectrometer (EA-IRMS, Thermo Fisher Flash HT 2000-Delta V plus) was used to determine the concentrations of particulate organic carbon (POC) and particulate organic nitrogen (PON) and their $\delta^{13}C$ and $\delta^{15}N$ values. The N₂ fixation and primary production rates were calculated according to Montoya et al. (1996) and Hama et al. (1983), respectively. The raw data and detailed information are shown in supporting information Data S1 and Text S1, respectively. To represent the inventories, the upper 100 m depth-integrated N₂ fixation (INF) and primary production (IPP) were

calculated by the trapezoidal integration method. The contributions of N₂ fixation-derived nitrogen to primary production are converted using Redfield ratio of 6.6 directly.

2.4. *nifH* Gene Abundance

The seawater samples for the *nifH* analyses were collected from 6 (SEATS, K8, N1, A3, D6, and F1) among the 19 stations. Briefly, 4 L of water sample was filtered onto 0.2- μm pore-sized membrane filters (Supor200, Pall Gelman, NY, USA) and then frozen in liquid N₂. To extract the DNA, membranes were cut into pieces under sterile conditions and then placed in tubes containing 800 μL of sucrose lysis buffer (40-mM EDTA, 50-mM Tris-HCl, 0.75-M sucrose) for bead beating using 0.1- and 0.5-mm glass beads. The cells were broken using a physical method, agitated for 3 min in a Fast Prep machine (MP Biomedicals, USA), and frozen in liquid nitrogen three times. Lysozyme (5 μL , 100 mgmL^{-1}) was then added, and the samples were incubated for 1 hr at 37 °C. After incubation, the lysate was transferred into a new 2-mL Eppendorf tube. Proteins were digested by incubation with 1% sodium dodecyl sulfate and proteinase K (250 μLmL^{-1}) at 55 °C for 2 hr and were removed by centrifuge at 12,000 g for 20 min at 4 °C after treatment with equal volumes of phenol:chloroform:isoamyl alcohol (25:24:1) containing 5-M NaCl. As a result, the samples were separated into three layers. The top aqueous layer containing genomic DNA was transferred into a new tube, to which an equal volume of chloroform:isoamyl alcohol (24:1) was added, followed by centrifugation at 12,000 g for 20 min at 4 °C. Genomic DNA was purified by precipitation with 100% isopropanol at -20 °C overnight, followed by washing with 70% ethanol and air drying. Genomic DNA was then eluted into 50- μL TE buffer and stored at -20 °C.

The quantitative polymerase chain reaction (qPCR) analysis was targeted on the *nifH* phylotypes of *Trichodesmium* spp., unicellular cyanobacterial UCYN-A1, UCYN-A2, and UCYN-B, *Richelia* spp. (het-1), and a gamma-proteobacterium (γ -24774A11) using previously designed primers and probe sets in supporting information Table S1 (Church, Jenkins, et al., 2005; Church, Short, et al., 2005; Foster et al., 2007; Langlois et al., 2008; Moisander et al., 2008; Thompson et al., 2014). The *nifH* standards were obtained by cloning the environmental sequences from previous samples of the SCS (Table S1). qPCR analysis was carried out as described previously (Church, Jenkins, et al., 2005) with slight modifications. Each 20- μL reaction mixture contained 2 μL 10 \times TaqMan[®] PCR buffer (Tiangen[®]), 250 μmolL^{-1} dNTP mixture, 250 nmolL^{-1} of fluorogenic probe, 250 nmolL^{-1} each of the forward and reverse primers, 0.5 U Taq DNA polymerase (Tiangen[®]) and 5 μL of environmental DNA or standard. Triplicate qPCR reactions were run for each environmental DNA sample and for each standard on a CFX96 Real-Time System (Bio-Rad Laboratories). The thermal cycle program was 50 °C for 2 min and 94 °C for 10 min, followed by 49 cycles of 95 °C for 15 s, 60 °C for 1 min. Standards corresponding to between 5×10^1 and 5×10^9 copies per well were amplified in the same 96-well plate. The copy numbers of the target genes in the environmental samples were calculated from the standard curve (supporting information Table S2). The Ct values of nontarget template were all less than the Ct value corresponding to 5×10^1 *nifH* copies for *Trichodesmium* (34.1), UCYN-A1 (36.1), UCYN-A2 (34.9), UCYN-B (34.9), het-1 (36.1), and γ -24774A11 (35.9). The detection limit of the qPCR reaction corresponded to around 50 *nifH* gene copies per PCR reaction, which was equivalent to around 625 gene copies per liter of seawater depending on the volume of seawater sample filtered (4 L). The efficiency of the PCR reaction varied between 90.3% and 95.3% (mean 93.1%).

2.5. Statistical Analysis

Statistical significance was tested using a *t* test, with values of $p < 0.05$ considered significant.

3. Results

3.1. Environmental Conditions

High-temperature, high-salinity water was found in the eastern part of NSCS, which is near the Luzon Strait, specifically at given depth of isopycnal surface of the potential density anomaly (σ) of 23 and 24 kgm^{-3} (supporting information Figure S2). This distribution pattern indicates a clear intrusion of Kuroshio deep into the NSCS during the time we made our survey. In addition, the contours of the depth of the isopycnal layer (Figure S2) showed a shoaling pattern toward the west, agreeing with previous findings that the SCS is a basin-scale upwelling system (Wong et al., 2007).

Table 1*Fundamental Parameters (Averaged Values) for the KI-Affected Region and the NSCS Region*

Parameter	KI-affected stations ($n = 6$)	NSCS stations ($n = 13$)	p value
Sea surface temperature (SST, °C)	28.9 ± 0.8	29.7 ± 0.4	0.009**
Sea surface salinity (SSS)	34.53 ± 0.05	34.20 ± 0.25	<0.001**
MLD (m)	26.2 ± 3.6	19.0 ± 4.3	0.003**
Nitracline depth (m)	45.4 ± 20.5	42.5 ± 13.3	0.726
Surface Chla ($\mu\text{g L}^{-1}$)	0.28 ± 0.09	0.23 ± 0.07	0.191
Integrated NO_x (INO_x , mmol m^{-2})	159 ± 60	256 ± 107	0.112
Integrated SRP (ISRP, mmol m^{-2})	14.6 ± 3.4	19.1 ± 7.5	0.238
INO_x :ISRP	10.8 ± 2.8	13.2 ± 0.8	0.046*
Surface N_2 fixation ($\text{nmol N} \cdot \text{L}^{-1} \cdot \text{day}^{-1}$)	8.5 ± 4.1	1.0 ± 0.7	0.007**
Surface primary production ($\mu\text{mol C} \cdot \text{L}^{-1} \cdot \text{day}^{-1}$)	0.45 ± 0.20	0.38 ± 0.13	0.382
INF ($\mu\text{mol N} \cdot \text{m}^{-2} \cdot \text{day}^{-1}$)	463 ± 260	50 ± 19	0.011*
IPP ($\text{mmol C} \cdot \text{m}^{-2} \cdot \text{day}^{-1}$)	61.5 ± 19.5	27.9 ± 10.4	<0.001**
INF N contribution to IPP (%)	5.1 ± 2.5	1.3 ± 0.5	0.012*

Note. The Equal Variance Test was conducted using Brown-Forsythe method, with $p > 0.05$ equal variance assumed. Student's t test ($p > 0.05$) or Welch's t test ($p < 0.05$) were conducted to compare the difference between the KI-affected stations and the NSCS stations. INF = integrated N_2 fixation; IPP = integrated; primary production; KI = Kuroshio intrusion; NSCS = northern South China Sea; SST = sea surface temperature; SSS = sea surface salinity; MLD = mixed layer depth; SRP = soluble reactive phosphorus.

* $p < 0.05$. ** $p < 0.01$.

In the θ - S diagram (Figure 1b), almost all of our sampling stations fell within the range of the two end-members. The spatial distribution of the KI index showed a tongue-like pattern revealing the KI pathway (Figure 1a), with a much higher $R_{\text{kave-100}}$ (>0.5) at stations close to the Luzon Strait (D4, D6, F1, F3, F7, and A3), which we defined as the KI-affected region. The remaining 13 stations with lower $R_{\text{kave-100}}$ (<0.5) were located in the NSCS region (SEATS, K2 to K8, A6, A9, A10, N1, and E4).

The fundamental parameters are presented as the averaged values in Table 1 for the comparison of the NSCS and KI-affected regions. The mean sea surface temperature and sea surface salinity showed a significant difference between the two regions, with an average 0.8 °C lower sea surface temperature and a slightly higher sea surface salinity (on average 0.33) in the KI-affected stations relative to the NSCS stations (Table 1). The MLD also revealed a significant difference between the KI-affected (26.2 ± 3.6 m) and the NSCS region (19.0 ± 4.3 m).

In the upper 25 m, both concentrations of NO_x and SRP were below the detection limit for all stations, while vertically, the concentration of nutrients increased with depth (Figure 2). The average depth of the nitracline

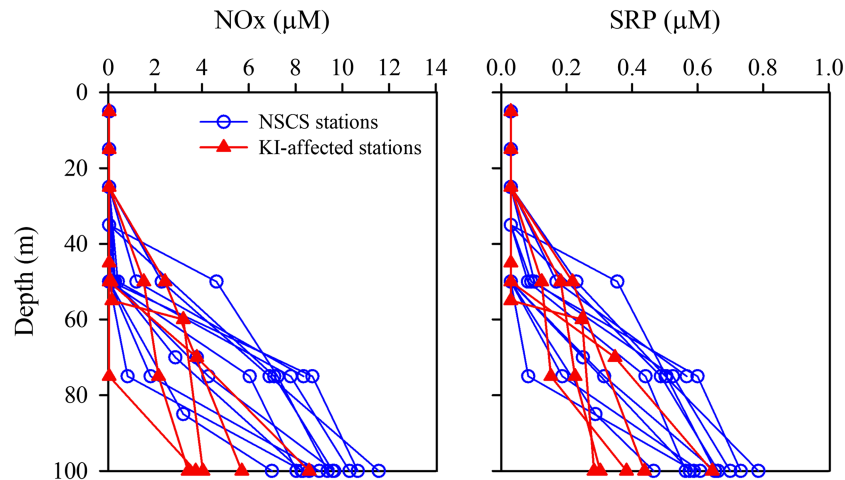


Figure 2. The vertical profiles of NO_x and SRP concentration (μM) at incubation stations. SRP = soluble reactive phosphorus; NSCS = northern South China Sea; KI = Kuroshio intrusion.

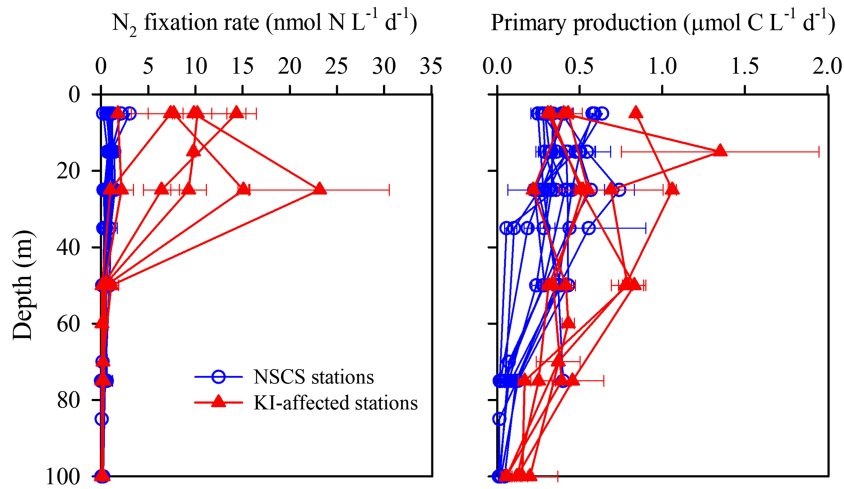


Figure 3. The vertical profiles of N_2 fixation rate ($\text{nmol N}\cdot\text{L}^{-1}\cdot\text{d}^{-1}$) and primary production ($\mu\text{mol C}\cdot\text{L}^{-1}\cdot\text{d}^{-1}$) at incubation stations. NSCS = northern South China Sea; KI = Kuroshio intrusion.

in the KI-affected region (45.4 ± 20.5 m) showed no difference from the NSCS region (42.5 ± 13.3 m). In general, the nutrient concentrations at the depths below the 50 m were higher in the NSCS region than in the KI-affected (Figure 2). No significant difference of the upper 100 m depth-integrated NO_x and SRP concentration was found between the NSCS region and the KI-affected region (t test $p > 0.05$, Table 1). However, the average concentration of integrated NO_x in the NSCS region (256 ± 107 $\text{mmol}\cdot\text{m}^{-2}$) was higher than in the KI-affected region (159 ± 60 $\text{mmol}\cdot\text{m}^{-2}$). No significant difference of depth-integrated SRP concentration was found between regions. The ratio of depth-integrated NO_x to SRP in the NSCS (13.2 ± 0.8) region was significantly higher (t test, $p = 0.046$) than that observed in the KI-affected region (10.8 ± 2.8 , Table 1), showing N deficit of upper 100 m in the KI-affected region. The sea surface Chl a concentration ranged from 0.16 to 0.4 $\mu\text{g}\cdot\text{L}^{-1}$, showing no difference between the two regions (Table 1).

3.2. Horizontal and Vertical Distributions of N_2 Fixation and Primary Production

The surface (5 m) N_2 fixation rate ranged from 1.8 to 14.3 $\text{nmol N}\cdot\text{L}^{-1}\cdot\text{day}^{-1}$, with an average of 8.5 ± 4.1 $\text{nmol N}\cdot\text{L}^{-1}\cdot\text{day}^{-1}$ in the KI-affected region, which was significantly higher than that observed in the NSCS region (in average 1.0 ± 0.7 $\text{nmol N}\cdot\text{L}^{-1}\cdot\text{day}^{-1}$, t test, $p < 0.001$, Figure 3 and Table 1). The surface primary production ranged from 0.25 to 0.84 $\mu\text{mol C}\cdot\text{L}^{-1}\cdot\text{day}^{-1}$ and showed no visible difference between the KI-affected and the NSCS region (Figure 3 and Table 1). Vertically, the relatively high rates of N_2 fixation and primary production were found in the upper 30 m, while below 30 m, the rates dropped rapidly (Figure 3). The INF in the KI-affected region (ranging from 105 to 885 $\mu\text{mol N}\cdot\text{m}^{-2}\cdot\text{day}^{-1}$ with an average of 463 ± 260 $\mu\text{mol N}\cdot\text{m}^{-2}\cdot\text{day}^{-1}$) were significantly higher than these in the NSCS region (from 29 to 89 $\mu\text{mol N}\cdot\text{m}^{-2}\cdot\text{day}^{-1}$ with an average 50 ± 19 $\mu\text{mol N}\cdot\text{m}^{-2}\cdot\text{day}^{-1}$, t test, $p < 0.05$, Figure 4a and Table 1). Although the surface primary production showed no noticeable difference between the KI-affected and NSCS region, the IPP were twice as high in the KI-affected region (average 61.5 ± 19.5 $\text{mmol C}\cdot\text{m}^{-2}\cdot\text{day}^{-1}$) than in the NSCS region (average 27.9 ± 10.4 $\text{mmol C}\cdot\text{m}^{-2}\cdot\text{day}^{-1}$, t test, $p < 0.001$, Figure 4b and Table 1).

3.3. Contribution of N_2 Fixation to N Demand of Primary Production

The percent contribution of N_2 fixation to the N demand of primary production was estimated based on a C:N ratio of 6.6. The vertical profile revealed opposite patterns between the KI-affected and NSCS regions (Figure 5). N_2 fixation contributed up to 22.0% of the N demand of primary production in the surface water at F3, and the contributions declined to a limited level at or below 50 m. The contributions were significantly higher in the KI-affected region (average 12.8% and 11.2% at 5 and 25 m, respectively) than in the NSCS region (average 1.4% and 1.8% at 5 and 25 m, respectively) at depths of 5 and 25 m (t test, $p < 0.05$). At 50 m or below, the fractional contribution decreased to $<2\%$ in the KI-affected region. In the NSCS region, the contribution increased with depth (up to 13.1% at 100 m at A10), and the average contribution at deeper depths was much higher than the contribution in the corresponding layer in the KI-affected region

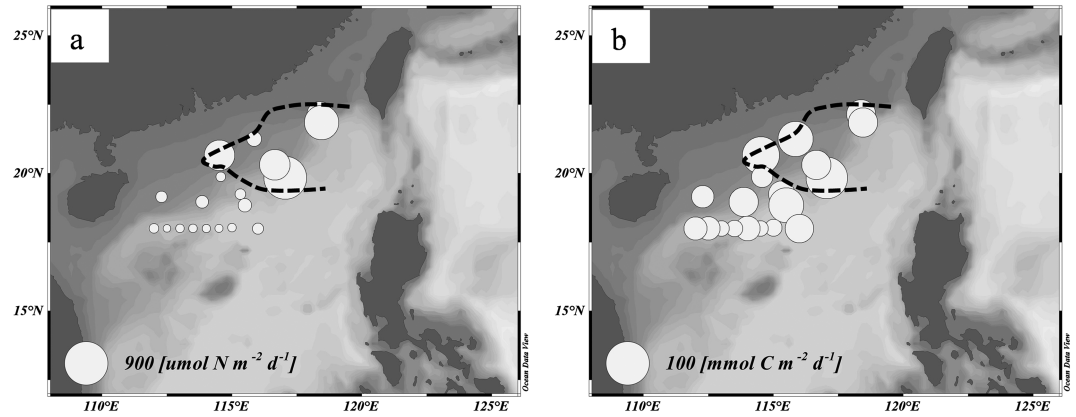


Figure 4. Spatial distributions of (a) the depth-integrated N_2 fixation rate ($\mu\text{mol N}\cdot\text{m}^{-2}\cdot\text{day}^{-1}$) and (b) depth-integrated primary production ($\text{mmol C}\cdot\text{m}^{-2}\cdot\text{day}^{-1}$). The dashed curves represent the isopleth of Kuroshio intrusion index of 0.5.

(Figure 5). Overall, the INF accounted for <8.2% of the N demand of the IPP at all stations in this study. The collective contribution of N_2 fixation was significantly higher in the KI-affected region ($5.1 \pm 2.5\%$) than in the NSCS region ($1.3 \pm 0.5\%$, t test, $p = 0.012$, Table 1).

3.4. Distribution of *nifH* Abundance

The diazotroph groups targeted by qPCR assays were detected at six stations, except for het-1, which was undetectable in all depths (Figure 6). *Trichodesmium* was nearly uniformly distributed from surface to 25 m and generally decreased at the depth below 50 m (Figure 6). Instead, unicellular cyanobacterial diazotrophs were most abundant in the subsurface water (25 or 50 m), where UCYN-A1 reached 7.1×10^4 to 3.7×10^5 *nifH* gene copies L^{-1} . The *nifH* of γ -24774A11 was observed from the surface to the depth of 100 m, and the abundance at depths showed relatively constant at around 10^4 copies L^{-1} in the upper 100 m (Figure 6).

Trichodesmium dominated the diazotrophic phylotypes throughout the water column in the KI-affected stations (A3, D6, and F1, Figure 6). The depth-integrated abundance was 2–4 orders of magnitude greater than that of the other phylotypes (contributed >98% of total gene abundance) and was 1–2 orders of magnitude higher than the *Trichodesmium* abundance in the NSCS stations (SEATS, K8, and N1, Table 2, t test $p = 0.048$).

The depth-integrated abundance of unicellular cyanobacterial diazotrophs (UCYN-A1, UCYN-A2, and UCYN-B) and γ -24774A11 revealed no significant difference between the NSCS region and KI-affected region (Table 2, t test, $p > 0.05$). In contrast to the KI-affected region, unicellular cyanobacterial diazotrophs contributed substantial portions at stations SEATS and K8 (45.3% and 56.1%, respectively).

4. Discussion

4.1. N_2 Fixation in the KI-Affected and NSCS Region

Kuroshio water, with a higher temperature and salinity, is well known to hold relatively low inorganic nutrients but high organic nutrients in the upper water compared to the central NSCS (Du et al., 2013; Wu et al., 2015). Thus, the intrusion of Kuroshio would substantially alter the nutrient inventory and subsequently the biogeochemical cycles in the NSCS (Du et al., 2013; Wu et al., 2015; Xu et al., 2018).

In our study, the surface N_2 fixation rates in the KI-affected region were significantly higher than the rates in the NSCS region (Figure 3). The average INF, $463 \pm 260 \mu\text{mol N}\cdot\text{m}^{-2}\cdot\text{day}^{-1}$, fell within the upper range of 100–1,000 $\mu\text{mol N}\cdot\text{m}^{-2}\cdot\text{day}^{-1}$ in the N_2 fixation

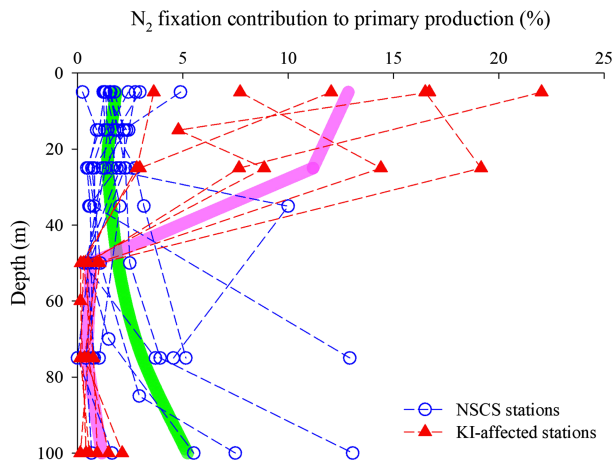


Figure 5. The depth distribution of N_2 fixation contribution to the N demand of primary production based on Redfield ratio of 6.6. The green and pink lines represent the average contribution of N_2 fixation to primary production in the NSCS region and KI-affected region, respectively. NSCS = northern South China Sea; KI = Kuroshio intrusion.

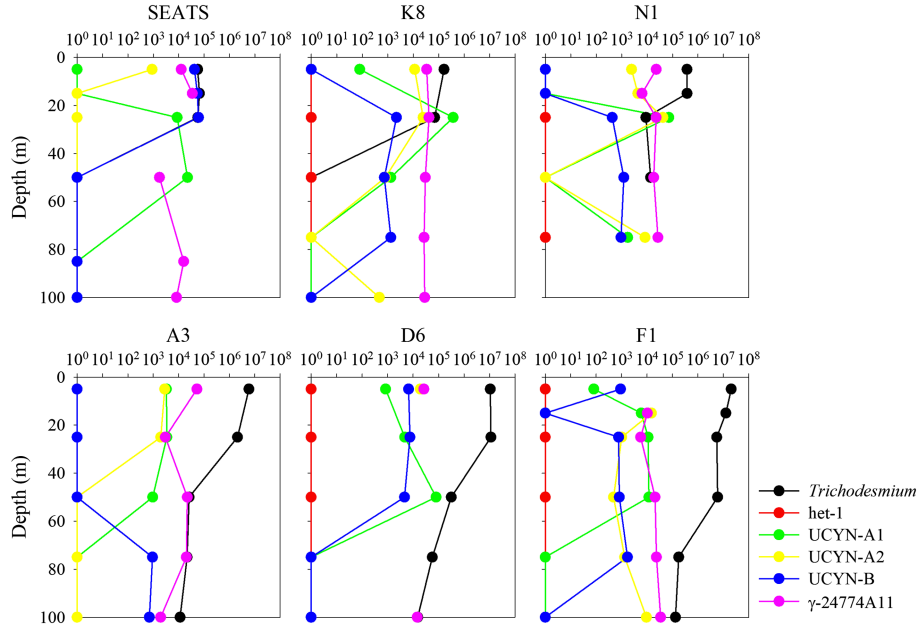


Figure 6. The vertical profiles of *nifH* phylotype abundances (*nifH* gene copies L⁻¹) at stations SEATS, K8, and N1 in the northern South China Sea (upper panels) and stations A3, D6, and F1 in the Kuroshio intrusion-affected region (lower panels).

database compiled by Luo et al. (2012) and much higher than that in typical oligotrophic gyre ocean (Dore et al., 2002; Falcon et al., 2004; Knapp et al., 2016; Moore et al., 2009; Table 3). In addition, the rates resembled that in the downstream Kuroshio near Japan, ALOHA station, and the western tropical South Pacific, regions considered “hot spots” for nitrogen fixation (Berthelot et al., 2017; Bonnet et al., 2015, 2017; Böttjer et al., 2016; Shiozaki et al., 2010, 2015). The “KI-affected” region in our study was in the region Lee Chen et al. (2014) defined as “NSCS basin”. To date, such high rate of nitrogen fixation in this region has not been reported previously, and the mean value was 1 order of magnitude higher than Lee Chen et al. (2014) reported (average $52 \pm 6 \mu\text{mol N}\cdot\text{m}^{-2} \text{day}^{-1}$). The difference in N₂ fixation rates between Lee Chen et al. (2014) and our study is probably due to the method inconsistency in N₂ fixation measurement. In the study conducted by Lee Chen et al. (2014), ¹⁵N₂ gas was injected directly before the incubation for N₂ fixation. Recent studies have demonstrated that nitrogen fixation activity determined by the gas bubble addition method could be >50% underestimated compared with that estimated by the ¹⁵N₂ dissolution method (Grosskopf et al., 2012; Mohr et al., 2010). Nevertheless, even the methodology was considered, no more than 10% of the N₂ fixation difference between studies can be explained. Therefore, other factors rather than methodology contributed to the high N₂ fixation rates in the KI-affected region, as well as the 1 order of magnitude higher rates compared to the NSCS region, during our investigation

Table 2

Depth-Integrated (upper 100 m) Gene Abundances of Five nifH Phylotypes of Dizaotroph at Six Stations We Surveyed (A3, D6, and F1 for KI-affected stations; SEATS, K8, N1 for NSCS Background Stations)

Station	<i>Trichodesmium</i>	UCYN-A1	UCYN-A2	UCYN-B	γ-24774A11
SEATS	2.21×10^9	8.28×10^8	8.93×10^6	2.02×10^9	1.24×10^9
K8	4.00×10^9	8.35×10^9	7.51×10^8	1.01×10^8	3.21×10^9
N1	3.20×10^{10}	1.27×10^9	9.03×10^8	4.96×10^7	1.48×10^9
A3	1.37×10^{11}	1.50×10^8	8.69×10^7	3.22×10^7	1.93×10^9
D6	4.24×10^{11}	2.12×10^9	2.88×10^8	3.22×10^7	5.79×10^8
F1	5.84×10^{11}	5.51×10^8	3.31×10^8	8.58×10^7	1.74×10^9

Note. The het-1 *nifH* gene abundances were undetectable at all stations. KI = Kuroshio intrusion; NSCS = northern South China Sea.

Table 3*The Reported N Fluxes in Global Ocean and Measured INF in This Study ($\mu\text{mol N}\cdot\text{m}^{-2}\cdot\text{day}^{-1}$)*

Region	Research type	Flux or INF	Reference
NSCS basin	N ₂ fixation	45.3 ± 6.2	Lee Chen et al. (2014)
Kuroshio upstream	N ₂ fixation	180.5 ± 34.3	Lee Chen et al. (2014)
Kuroshio downstream	N ₂ fixation	199 ± 142	Shiozaki et al. (2015)
NSCS basin	N ₂ fixation	50 ± 19	this study
KI-affected NSCS	N ₂ fixation	463 ± 260	this study
ALOHA	N ₂ fixation	230 ± 136	Böttjer et al. (2016)
North Pacific Ocean	N ₂ fixation	30–120	Dore et al. (2002)
South Pacific Ocean	N ₂ fixation	23–98	Knapp et al. (2016)
Tropical North Atlantic Ocean	N ₂ fixation	73–90	Falcon et al. (2004)
South Atlantic Ocean	N ₂ fixation	~20	Moore et al. (2009)
NSCS basin	Atmospheric deposition	20–150	Kao et al. (2012), Kim et al. (2014), Yang et al. (2014)
NSCS basin	Export PON flux	365–650	Cai et al. (2015), Chen et al. (1998)
Kuroshio upstream	Export PON flux	350–600	Hung and Gong (2007)

Note. INF = depth-integrated N₂ fixation; KI = Kuroshio intrusion; NSCS = northern South China Sea; PON = particulate organic nitrogen.

(Figures 3 and 4). Lee Chen et al. (2014) found that the INF in the main stream Kuroshio was several times higher than that in the NSCS basin. They suggested that the much deeper nitracline in the upstream Kuroshio might provide a suitable condition for diazotrophs competing for nutrients (such as Fe and P) with fast-growth nondiazotrophs (Lee Chen et al., 2003, 2008, 2014). In addition, bio-essential Fe sourced from the islands upstream (Aguilar-Islas et al., 2007; Blain et al., 2007) and the continental shelf due to sediment resuspension and pore water diffusion (Bruland et al., 2005; Lam & Bishop, 2008), probably promote diazotrophic abundance and activity along the Kuroshio Current (Shiozaki et al., 2015). Thus, the high rates of N₂ fixation appeared in the KI-affected region probably due to the lateral transport from the main stream of the Kuroshio.

4.2. Advection of *Trichodesmium* to the NSCS

In the NSCS region, other diazotrophic phylotypes rather than *Trichodesmium* dominated the *nifH* gene abundance at stations SEATS and K8. The unicellular cyanobacterial diazotrophs (UCYN-A1, UCYN-A2, and UCYN-B) account for around half of the total gene abundance, while the *Trichodesmium* and γ -24774A11 composed less than 30%, respectively (Table 2). The result was consistent to previous findings that unicellular cyanobacterial diazotrophs were the major contributors to the N₂ fixation in the NSCS

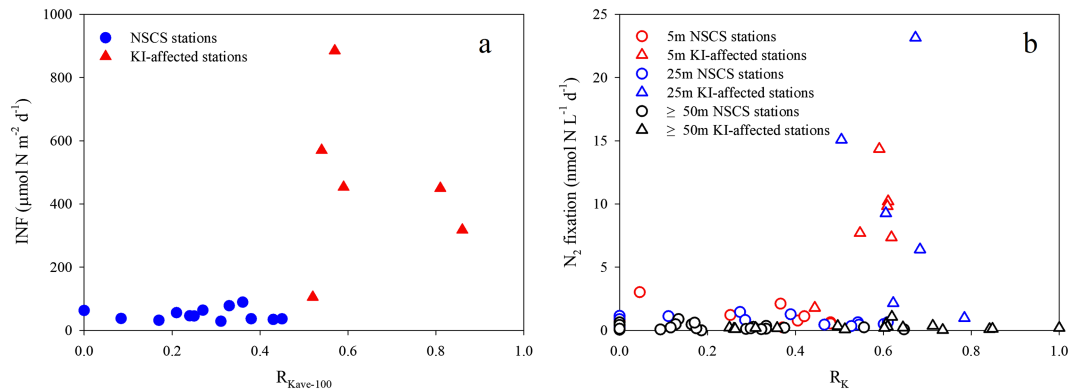


Figure 7. (a) The depth-integrated (upper 100 m) N₂ fixation rate (INF, $\mu\text{mol N}\cdot\text{m}^{-2}\cdot\text{day}^{-1}$) against the average Kuroshio fraction in the upper 100 m; (b) N₂ fixation rate (nmol N·L⁻¹·day⁻¹) against the Kuroshio fraction at each depth (5, 25, and 50 m). NSCS = northern South China Sea; KI = Kuroshio intrusion.

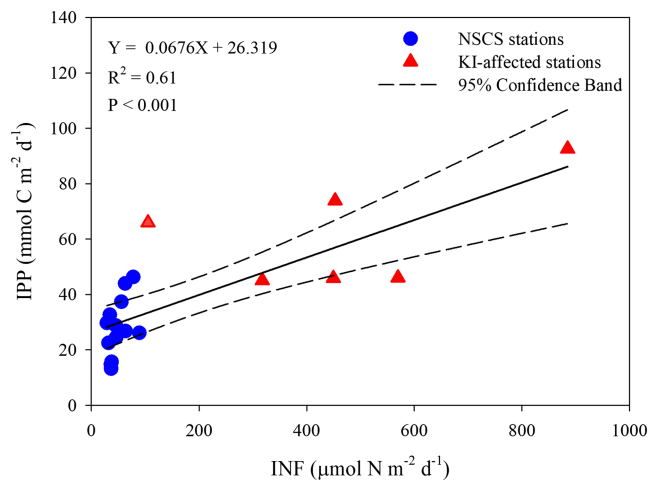


Figure 8. Linear correlation between INF and IPP for all 19 stations. Solid triangles represent the KI-affected stations, while the solid circles represent the NSCS stations. NSCS = northern South China Sea; KI = Kuroshio intrusion; INF = integrated N_2 fixation; IPP = integrated primary production.

(Lee Chen et al., 2014; Wong et al., 2015). In addition to unicellular cyanobacterial diazotrophs, proteobacteria was also found to be a potential N_2 fixation contributor in the SCS (Kong et al., 2011; Zhang et al., 2011). The absolute depth-integrated abundances of UCYN-A1, UCYN-A2, UCYN-B, and γ -24774A11 revealed no significant difference between the NSCS region and KI-affected region (Table 2). In contrast, Shiozaki, Lee Chen, et al. (2014) found orders of magnitude higher of UCYN-B abundance in the main stream of Kuroshio in summer than that in NSCS. During our cruise, we did not investigate the stations in the main stream Kuroshio. Thus, we are not sure whether there is a high abundance of UCYN-B in the Kuroshio as found by Shiozaki, Lee Chen, et al. (2014). Nevertheless, the intrusion of Kuroshio likely creates a new biogeographic regime in the front zone suitable for the growth of *Trichodesmium*.

The orders of magnitude higher *Trichodesmium* abundance in the KI-affected region relative to the NSCS background strongly suggests the observed high N_2 fixation rates was attributed to *Trichodesmium* brought by the Kuroshio. In the oligotrophic ocean, *Trichodesmium*

often formed extensive bloom in stratified water with low turbulence, slow NO_3^- input from deep water, and a sufficient supply of Fe and P (Capone et al., 1997). Thus, the environmental conditions in the Kuroshio might suitable for *Trichodesmium*. Indeed, *Trichodesmium* dominated the diazotrophic community in the main stream of Kuroshio, especially around islands (Lee Chen et al., 2003; Shiozaki et al., 2015). Given its buoyant feature, the distribution pattern of *Trichodesmium* can be regulated by the ocean currents. For example, *Trichodesmium* in the western subtropical North Atlantic can be transported by the Gulf Stream to the high-latitude regions (Lipschultz & Owens, 1996). Similarly, *Trichodesmium* flourished around islands in upper stream of the Kuroshio can be transported to the downstream region near Japan (Shiozaki et al., 2015). Thus, we infer that the high abundance of *Trichodesmium* in KI-affected region during our study may be transported from the main stream of Kuroshio during the intrusion events, which significantly enhance the N_2 fixation rate in the regions with $R_k > 0.5$ (Figures 4 and 7). However, we found higher INF values with higher KI index, yet the highest INF did not appear at the Kuroshio end (Figure 7a). Since the majority of the N_2 fixation had occurred in the surface 30 m, we combined the measurements of the corresponding layers for comparison (Figure 7b) and found that the high N_2 fixation values located at KI index are around 0.6 in the surface 5 and 25 m. Either we missed sampling the surface waters from regions with high KI index during our cruise or some other process further amplified the nitrogen fixation in the shallow water at stations with R_k of around 0.5–0.6. Our results demonstrated that diazotrophs (mainly *Trichodesmium*) and high N_2 fixation were tightly associated with the KI, which modulated the biogeographic distribution of N_2 fixers.

To better estimate the global N_2 fixation budget and understand the role of N_2 fixation in the biogeochemical cycles of complicated physical domains, further studies are required to explore the influence of this kind of boundary current effect and its spreading capacity and the biogeochemical behavior therein. Further isotope and molecular level studies are needed to constrain the internal mechanisms to stimulate on-site N_2 fixation or to sustain diazotrophs over long-distance travel.

4.3. Linkage Between Nitrogen Fixation, New Production and Primary Production

Linking to the biological pump, the amount of N_2 fixation was comparable with previously reported export production, accounting for 50–100% of the export production in the NSCS euphotic zone (Cai et al., 2015; Chen et al., 1998, 2008; Table 3). Such a high contribution suggests that N_2 fixation associated with the KI alone may play a considerable role in the biogeochemical cycles of carbon and nitrogen in the SCS.

Relative to the diapycnal supply of dissolved inorganic nitrogen ($\sim 110 \mu\text{mol N}\cdot\text{m}^{-2}\cdot\text{day}^{-1}$) to the euphotic zone observed previously at SEATS (Du et al., 2017), the water column INF rates were much lower in the NSCS region ($\sim 50 \mu\text{mol N}\cdot\text{m}^{-2}\cdot\text{day}^{-1}$). In contrast, the INF was ~ 4 times higher in the KI-affected region,

as high as $460 \mu\text{mol N}\cdot\text{m}^{-2}\cdot\text{day}^{-1}$. Such high INF rates demonstrate the significance of the lateral input of new nitrogen induced by diazotrophs. It also suggests that the primary producers in the KI-affected region benefitted from the nitrogen input via diazotrophs during our sampling period.

A significant positive correlation was obtained between the INF and the IPP across the 19 research stations (Figure 8, $R^2 = 0.61$, $p < 0.001$). The high INF is accompanied with relatively high IPP in the KI-affected region, implying the potential role of diazotrophs in the primary productivity. Our result was in line with the findings of previous mesocosm studies, in which higher primary production was associated with higher N_2 fixation (Berthelot et al., 2015; Van Wambeke et al., 2016). Similarly, in field studies, N_2 fixation were reported to have a positive linear relationship with primary production regardless surface or water column integrated (Bonnet et al., 2015; Shiozaki et al., 2018).

As indicated in Figure 5, the N_2 fixers were not the mainly contributor of primary production. Assuming that most N_2 fixation activity was contributed by cyanobacterial diazotrophs, collectively, the measured INF in the upper 100 m may only account for $\sim 1.3\%$ of the N demand of IPP in the NSCS region and $\sim 5.1\%$ in the KI-affected region, despite the maximum contribution reaching as high as $\sim 22\%$ in the surface water (Figure 5). It is likely that additional nitrogen sources associated with *Trichodesmium* activity generated a linear correlation between INF and IPP.

Principally, *Trichodesmium* has been shown to release a substantial portion (up to 90%) of newly fixed nitrogen to the dissolved pool and transfer it to nondiazotrophs in the short term (24 hr; Bonnet et al., 2016; Lee Chen et al., 2011; Mulholland & Bernhardt, 2005). This new bioavailable nitrogen derived from *Trichodesmium* may accumulate and substantially enhance regenerated production in the euphotic zone (Shiozaki et al., 2018). In many previous studies, bacterial production was limited by lack of bioavailable N. Thus, the accumulated newly fixed nitrogen, on the other hand, may stimulate bacterial production, which could degrade more dissolved organic matter into bioavailable N and relax the N limitation for primary producers in the euphotic zone (Berthelot et al., 2015; Van Wambeke et al., 2016). At depths below 25 m, the contribution of N_2 fixation to primary production declined quickly to a level of $< 2\%$ at the depth of 50 m in the KI-affected region (Figure 5). Although most N_2 fixation and primary production both are light driven in euphotic zone, under low-light stress, *Trichodesmium* physiologically preferred to allocate more energy for carbon fixation to alleviate the intensive carbon consumption by respiration, thus nearly shutting down N_2 fixation at depths below 50 m (Lu et al., 2018). On the other hand, low-light stress may further enhance the diazotrophic-derived nitrogen release by *Trichodesmium* to the surrounding water directly or indirectly (Bonnet et al., 2016; Lu et al., 2018; Mulholland et al., 2004). Although not settled, three mechanisms (diazotrophic-derived nitrogen release, new nitrogen accumulation, and stimulation of heterotrophic bacterial productivity) are offered here to explain the linear relationship between INF and IPP and to address the role of *Trichodesmium* in the coupled nitrogen and carbon cycle from a biogeochemical perspective.

In the NSCS region, the opposite vertical pattern of N_2 fixation contribution to the N demand of primary production was probably induced by the distinct diazotrophic abundance and community structure (Figures 5 and 6). Apparently, the total primary production in the NSCS region was mainly maintained by the N flux from the deep water (Lee Chen et al., 2008), thus, diazotrophs may play a minor role in carbon fixation. Unicellular cyanobacterial diazotrophs and proteobacterium were the dominant diazotrophic species at station SEATS and K8, which most likely support the observed N_2 fixation (Table 2). The fate of dinitrogen fixed by unicellular cyanobacterial diazotrophs and proteobacterium is not well understood. Among which, the unicellular cyanobacterial UCYN-A lacks key genes for carbon fixation and thus lives in symbioses with specific eukaryotic algae (Bombar et al., 2014; Tripp et al., 2010). It is known that dinitrogen fixed by UCYN-A efficiently transferred to its host (Martinez-Perez et al., 2016), and thus the surrounding planktonic communities may not benefit from this new nitrogen directly in short term (Shiozaki et al., 2018).

5. Conclusions

The seasonal intrusion of the western boundary Kuroshio Current into the SCS may not only influence the nutrient structure but also the community of diazotrophs, the N_2 fixation rate, and primary productivity as well. Our findings provide clues to linking the physical circulation pattern to biogeochemistry and

demonstrate that the western boundary current could effectively spread the active *Trichodesmium*-dominated N₂-fixation signal widely. Meanwhile, a significant positive correlation between N₂ fixation and primary productivity shows that N₂ fixation is tightly tied to marine carbon cycling, although the mechanisms remain unresolved.

References

- Aguilar-Islas, A. M., Hurst, M. P., Buck, K. N., Sohst, B., Smith, G. J., Lohan, M. C., & Bruland, K. W. (2007). Micro- and macronutrients in the southeastern Bering Sea: Insight into iron-replete and iron-depleted regimes. *Progress in Oceanography*, 73(2), 99–126. <https://doi.org/10.1016/j.pocean.2006.12.002>
- Bergman, B., Sandh, G., Lin, S., Larsson, J., & Carpenter, E. J. (2013). *Trichodesmium*—A widespread marine cyanobacterium with unusual nitrogen fixation properties. *FEMS Microbiology Reviews*, 37(3), 286–302. <https://doi.org/10.1111/j.1574-6976.2012.00352.x>
- Berthelot, H., Benavides, M., Moisan, P. H., Grosso, O., & Bonnet, S. (2017). High-nitrogen fixation rates in the particulate and dissolved pools in the western tropical Pacific (Solomon and Bismarck Seas). *Geophysical Research Letters*, 44, 8414–8423. <https://doi.org/10.1002/2017gl073856>
- Berthelot, H., Moutin, T., L'Helguen, S., Leblanc, K., Hélias, S., Grosso, O., et al. (2015). Dinitrogen fixation and dissolved organic nitrogen fueled primary production and particulate export during the VAHINE mesocosm experiment (New Caledonia lagoon). *Biogeosciences*, 12(13), 4099–4112. <https://doi.org/10.5194/bg-12-4099-2015>
- Blain, S., Quéguiner, B., Armand, L., Belviso, S., Bombled, B., Bopp, L., et al. (2007). Effect of natural iron fertilization on carbon sequestration in the Southern Ocean. *Nature*, 446(7139), 1070–1074. <https://doi.org/10.1038/nature05700>
- Bombar, D., Heller, P., Sanchez-Baracaldo, P., Carter, B. J., & Zehr, J. P. (2014). Comparative genomics reveals surprising divergence of two closely related strains of uncultivated UCYN-A cyanobacteria. *The ISME Journal*, 8(12), 2530–2542. <https://doi.org/10.1038/ismej.2014.167>
- Bonnet, S., Berthelot, H., Turk-Kubo, K., Cornet-Barthaux, V., Fawcett, S., Berman-Frank, I., et al. (2016). Diazotroph derived nitrogen supports diatom growth in the South West Pacific: A quantitative study using nanoSIMS. *Limnology and Oceanography*, 61(5), 1549–1562. <https://doi.org/10.1002/lno.10300>
- Bonnet, S., Caffin, M., Berthelot, H., & Moutin, T. (2017). Hot spot of N₂ fixation in the western tropical South Pacific pleads for a spatial decoupling between N₂ fixation and denitrification. *PNAS*, 114, E2800–E2801. <https://doi.org/10.1073/pnas.1619514114>
- Bonnet, S., Rodier, M., Turk-Kubo, K. A., Germaineaud, C., Menkes, C., Ganachaud, A., et al. (2015). Contrasted geographical distribution of N₂ fixation rates and *nifH* phylotypes in the Coral and Solomon Seas (southwestern Pacific) during austral winter conditions. *Global Biogeochemical Cycles*, 29, 1874–1892. <https://doi.org/10.1002/2015gb005117>
- Borgen, R. L., Barber, R. T., Delcroix, T., Inoue, H. Y., Mackey, D. J., & Rodier, M. (2002). Pacific warm pool and divergence: Temporal and zonal variations on the equator and their effects on the biological pump. *Deep Sea Research*, 49(13-14), 2471–2512. [https://doi.org/10.1016/S0967-0645\(02\)00045-0](https://doi.org/10.1016/S0967-0645(02)00045-0)
- Böttjer, D., Dore, J. E., Karl, D. M., Letelier, R. M., Mahaffey, C., Wilson, S. T., et al. (2016). Temporal variability of nitrogen fixation and particulate nitrogen export at Station ALOHA. *Limnology and Oceanography*. <https://doi.org/10.1002/lno.10386>
- Bruland, K. W., Rue, E. L., Smith, G. J., & DiTullio, G. R. (2005). Iron, macronutrients and diatom blooms in the Peru upwelling regime: Brown and blue waters of Peru. *Marine Chemistry*, 93(2-4), 81–103. <https://doi.org/10.1016/j.marchem.2004.06.011>
- Cai, P., Zhao, D., Wang, L., Huang, B., & Dai, M. (2015). Role of particle stock and phytoplankton community structure in regulating particulate organic carbon export in a large marginal sea. *Journal of Geophysical Research: Oceans*, 120, 2063–2095. <https://doi.org/10.1002/2014JC010432>
- Capone, D. G., Burns, J. A., Montoya, J. P., Subramaniam, A., Mahaffey, C., Gunderson, T., et al. (2005). Nitrogen fixation by *Trichodesmium* spp.: An important source of new nitrogen to the tropical and subtropical North Atlantic Ocean. *Global Biogeochemical Cycles*, 19, GB2024. <https://doi.org/10.1029/2004GB002331>
- Capone, D. G., Zehr, J. P., Paerl, H. W., Badger, M. R., & Carpenter, E. J. (1997). *Trichodesmium*, a globally significant marine cyanobacterium. *Science*, 276, 1221–1229. <https://doi.org/10.1126/science.276.5316.1221>
- Chen, J., Zheng, L., Wiesner, M., Chen, R., Zheng, Y., & Wong, H. (1998). Estimations of primary production and export production in the South China Sea based on sediment trap experiments. *Chinese Science Bulletin*, 43(7), 583–586. <https://doi.org/10.1007/Bf02883645>
- Chen, W., Cai, P., Dai, M., & Wei, J. (2008). (234)Th/(238)U disequilibrium and particulate organic carbon export in the northern South China Sea. *Journal of Oceanography*, 64(3), 417–428. <https://doi.org/10.1007/s10872-008-0035-z>
- Church, M. J., Jenkins, B. D., Karl, D. M., & Zehr, J. P. (2005). Vertical distributions of nitrogen fixing phylotypes at Stn ALOHA in the oligotrophic North Pacific Ocean. *Aquatic Microbial Ecology*, 38, 3–14. <https://doi.org/10.3354/ame038003>
- Church, M. J., Short, C. M., Jenkins, B. D., Karl, D. M., & Zehr, J. P. (2005). Temporal patterns of nitrogenase gene (*nifH*) expression in the oligotrophic North Pacific Ocean. *Applied and Environmental Microbiology*, 71(9), 5362–5370. <https://doi.org/10.1128/AEM.71.9.5362-5370>
- Davis, C. S., & McGillicuddy, D. J. (2006). Transatlantic abundance of the N₂-fixing colonial cyanobacterium *Trichodesmium*. *Science*, 312(5779), 1517–1520. <https://doi.org/10.1126/science.1123570>
- Dore, J. E., Brum, J. R., Tupas, L. M., & Karl, D. M. (2002). Seasonal and interannual variability in sources of nitrogen supporting export in the oligotrophic subtropical North Pacific Ocean. *Limnology and Oceanography*, 47(6), 1595–1607. <https://doi.org/10.4319/lno.2002.47.6.1595>
- Du, C., Liu, Z., Dai, M., Kao, S. J., Cao, Z., Zhang, Y., et al. (2013). Impact of the Kuroshio intrusion on the nutrient inventory in the upper northern South China Sea: Insights from an isopycnal mixing model. *Biogeosciences*, 10, 1–14. <https://doi.org/10.5194/bg-10-1-2013>
- Du, C., Liu, Z., Kao, S. J., & Dai, M. (2017). Diapycnal fluxes of nutrients in an oligotrophic oceanic regime: The South China Sea. *Geophysical Research Letters*, 44, 11,510–11,518. <https://doi.org/10.1002/2017GL074921>
- Dupouy, C., Benielli-Gary, D., Neveux, J., Dandonneau, Y., & Westberry, T. K. (2011). An algorithm for detecting *Trichodesmium* surface blooms in the south western tropical Pacific. *Biogeosciences*, 8(12), 3631–3647. <https://doi.org/10.5194/bg-8-3631-2011>
- Falcon, L. I., Carpenter, E. J., Cipriano, F., Bergman, B., & Capone, D. G. (2004). N₂ fixation by unicellular bacterioplankton from the Atlantic and Pacific Oceans: Phylogeny and in situ rates. *Applied and Environmental Microbiology*, 70(2), 765–770. <https://doi.org/10.1128/aem.70.2.765-770>

Acknowledgments

We are grateful to National Natural Science Foundation of China (NSFC U1305233, 41376116, 41721005, and 91328207), National Key Basic Research Program of China (973 Program 2014CB953702 and 2015CB954003), and Scientific Research Fund of the Second Institute of Oceanography, SOA (SZ1914). Thanks for help from technicians Tian Li and Zou Wenbin in determination of POC and PON and their δ¹³C and δ¹⁵N values, who are in our Nitrogen Cycle Group at the State Key Laboratory of Marine Environmental Science (Xiamen University, China). Data sets for this paper are available in the supporting information.

- Fong, A. A., Karl, D. M., Lukas, R., Letelier, R. M., Zehr, J. P., & Church, M. J. (2008). Nitrogen fixation in an anticyclonic eddy in the oligotrophic North Pacific Ocean. *The ISME Journal*, 2(6), 663–676. <https://doi.org/10.1038/ismej.2008.22>
- Foster, R. A., Subramaniam, A., Mahaffey, C., Carpenter, E. J., Capone, D. G., & Zehr, J. P. (2007). Influence of the Amazon River plume on distributions of free-living and symbiotic cyanobacteria in the western tropical North Atlantic Ocean. *Limnology and Oceanography*, 52(2), 517–532. <https://doi.org/10.4319/lo.2007.52.2.0517>
- Grosskopf, T., Mohr, W., Baustian, T., Schunck, H., Gill, D., Kuypers, M. M. M., et al. (2012). Doubling of marine dinitrogen-fixation rates based on direct measurements. *Nature*, 488(7411), 361–364. <https://doi.org/10.1038/nature11338>
- Hama, T., Miyazaki, T., Ogawa, Y., Iwakuma, T., Takahashi, M., Otsuki, A., & Ichimura, S. (1983). Measurement of photosynthetic production of a marine phytoplankton population using a stable ^{13}C isotope. *Marine Biology*, 73(1), 31–36. <https://doi.org/10.1007/BF00396282>
- Hung, C. C., & Gong, G. C. (2007). Export flux of POC in the main stream of the Kuroshio. *Geophysical Research Letters*, 34, L18606. <https://doi.org/10.1029/2007GL030236>
- Kao, S. J., Yang, J. Y. T., Liu, K. K., Dai, M., Chou, W. C., Lin, H. L., & Ren, H. (2012). Isotope constraints on particulate nitrogen source and dynamics in the upper water column of the oligotrophic South China Sea. *Global Biogeochemical Cycles*, 26, GB2033. <https://doi.org/10.1029/2011GB004091>
- Kara, A. B., Rochford, P. A., & Hurlburt, H. E. (2000). An optimal definition for ocean mixed layer depth. *Journal of Geophysical Research*, 105(C7), 16803–16821. <https://doi.org/10.1029/2000JC900072>
- Kim, T. W., Lee, K., Duce, R., & Liss, P. (2014). Impact of atmospheric nitrogen deposition on phytoplankton productivity in the South China Sea. *Geophysical Research Letters*, 41, 3156–3162. <https://doi.org/10.1002/2014GL059665>
- Knapp, A. N., Casciotti, K. L., Berelson, W. M., Prokopenko, M. G., & Capone, D. G. (2016). Low rates of nitrogen fixation in eastern tropical South Pacific surface waters. *PNAS*, 113(16), 4398–4403. <https://doi.org/10.1073/pnas.1515641113>
- Kong, L., Jing, H., Kataoka, T., Sun, J., & Liu, H. (2011). Phylogenetic diversity and spatio-temporal distribution of nitrogenase genes (*nifH*) in the northern South China Sea. *Aquatic Microbial Ecology*, 65(1), 15–27. <https://doi.org/10.3354/ame01531>
- Lam, P. J., & Bishop, J. K. B. (2008). The continental margin is a key source of iron to the HNLC North Pacific Ocean. *Geophysical Research Letters*, 35, L07608. <https://doi.org/10.1029/2008GL033294>
- Langlois, R. J., Hummer, D., & LaRoche, J. (2008). Abundances and distributions of the dominant *nifH* phylotypes in the Northern Atlantic Ocean. *Applied and Environmental Microbiology*, 74(6), 1922–1931. <https://doi.org/10.1128/AEM.01720-07>
- Lee Chen, Y. L., Chen, H. Y., & Lin, Y. H. (2003). Distribution and downward flux of *Trichodesmium* in the South China Sea as influenced by the transport from the Kuroshio Current. *Marine Ecology Progress Series*, 259, 47–57. <https://doi.org/10.3354/meps259047>
- Lee Chen, Y. L., Chen, H. Y., Lin, Y. H., Yong, T. C., Taniuchi, Y., & Tuo, S. H. (2014). The relative contributions of unicellular and filamentous diazotrophs to N_2 fixation in the South China Sea and the upstream Kuroshio. *Deep Sea Research*, 85, 56–71. <https://doi.org/10.1016/j.dsr.2013.11.006>
- Lee Chen, Y. L., Chen, H. Y., Tuo, S. H., & Ohki, K. (2008). Seasonal dynamics of new production from *Trichodesmium* N_2 fixation and nitrate uptake in the upstream Kuroshio and South China Sea basin. *Limnology and Oceanography*, 53, 1705–1721. <https://doi.org/10.4319/lo.2008.53.5.1705>
- Lee Chen, Y. L., Tuo, S. H., & Chen, H. Y. (2011). Co-occurrence and transfer of fixed nitrogen from *Trichodesmium* spp. to diatoms in the low-latitude Kuroshio Current in the NW Pacific. *Marine Ecology Progress Series*, 421, 25–38. <https://doi.org/10.3354/meps08908>
- Lipschultz, F., & Owens, N. J. P. (1996). An assessment of nitrogen fixation as a source of nitrogen to the North Atlantic Ocean. *Biogeochemistry*, 35(1), 261–274. <https://doi.org/10.1007/Bf02179830>
- Lu, Y., Wen, Z., Shi, D., Chen, M., Zhang, Y., Bonnet, S., et al. (2018). Effect of light on N_2 fixation and net nitrogen release of *Trichodesmium* in a field study. *Biogeosciences*, 15(1), 1–12. <https://doi.org/10.5194/bg-15-1-2018>
- Luo, Y. W., Doney, S. C., Anderson, L. A., Benavides, M., Berman-Frank, I., Bode, A., et al. (2012). Database of diazotrophs in global ocean abundance, biomass and nitrogen fixation rates. *Earth System Science Data*, 4(1), 47–73. <https://doi.org/10.5194/essd-4-47-2012>
- Martinez-Perez, C., Mohr, W., Löscher, C. R., Dekaezemacker, J., Littmann, S., Yilmaz, P., et al. (2016). The small unicellular diazotrophic symbiont, UCYN-A, is a key player in the marine nitrogen cycle. *Nature Microbiology*, 1, 16163. <https://doi.org/10.1038/NMICROBIOL.2016.163>
- Mohr, W., Großkopf, T., Wallace, D. W., & LaRoche, J. (2010). Methodological underestimation of oceanic nitrogen fixation rates. *PLoS ONE*, 5(9), e12583. <https://doi.org/10.1371/journal.pone.0012583.g001>
- Moisander, P. H., Beinart, R. A., Voss, M., & Zehr, J. P. (2008). Diversity and abundance of diazotrophic microorganisms in the South China Sea during intermonsoon. *The ISME Journal*, 2(9), 954–967. <https://doi.org/10.1038/ismej.2008.51>
- Montoya, J. P., Voss, M., Kähler, P., & Capone, D. G. (1996). A simple, high-precision, high-sensitivity tracer assay for N_2 fixation. *Applied and Environmental Microbiology*, 62, 986–993.
- Moore, C. M., Mills, M. M., Arrigo, K. R., Berman-Frank, I., Bopp, L., Boyd, P. W., et al. (2013). Processes and patterns of oceanic nutrient limitation. *Nature Geoscience*, 6(9), 701–710. <https://doi.org/10.1038/ngeo1765>
- Moore, C. M., Mills, M. M., Achterberg, E. P., Geider, R. J., LaRoche, J., Lucas, M. I., et al. (2009). Large-scale distribution of Atlantic nitrogen fixation controlled by iron availability. *Nature Geoscience*, 2(12), 867–871. <https://doi.org/10.1038/ngeo667>
- Mourino-Carballido, B., Grana, R., Fernandez, A., Bode, A., Varela, M., Dominguez, J. F., et al. (2011). Importance of N_2 fixation vs. nitrate eddy diffusion along a latitudinal transect in the Atlantic Ocean. *Limnology and Oceanography*, 56(3), 999–1007. <https://doi.org/10.4319/lo.2011.56.3.0999>
- Mulholland, M. R., & Bernhardt, P. W. (2005). The effect of growth rate, phosphorus concentration, and temperature on N_2 fixation, carbon fixation. *Limnology and Oceanography*, 50, 839–849. <https://doi.org/10.4319/lo.2005.50.3.0839>
- Mulholland, M. R., Bronk, D. A., & Capone, D. G. (2004). Dinitrogen fixation and release of ammonium and dissolved organic nitrogen by *Trichodesmium* IMS101. *Aquatic Microbial Ecology*, 37, 85–94. <https://doi.org/10.3354/ame037085>
- Olson, E. M., McGillicuddy, D. J., Flierl, G. R., Davis, C. S., Dyhrman, S. T., & Waterbury, J. B. (2015). Mesoscale eddies and *Trichodesmium* spp. distributions in the southwestern North Atlantic. *Journal of Geophysical Research: Oceans*, 120, 4129–4150. <https://doi.org/10.1002/2015JC010728>
- Rijkenberg, M. J. A., Langlois, R. J., Mills, M. M., Patey, M. D., Hill, P. G., Nielsdottir, M. C., et al. (2011). Environmental forcing of nitrogen fixation in the eastern tropical and sub-tropical North Atlantic Ocean. *PLoS ONE*, 6(12), e28989. <https://doi.org/10.1371/journal.pone.0028989>
- Shiozaki, T., Bombar, D., Riemann, L., Sato, M., Hashihama, F., Kodama, T., et al. (2018). Linkage between dinitrogen fixation and primary production in the oligotrophic South Pacific Ocean. *Global Biogeochemical Cycles*, 32, 1028–1044. <https://doi.org/10.1029/2017GB005869>

- Shiozaki, T., Furuya, K., Kodama, T., Kitajima, S., Takeda, S., Takemura, T., & Kanda, J. (2010). New estimation of N₂ fixation in the western and central Pacific Ocean and its marginal seas. *Global Biogeochemical Cycles*, *24*, GB1015. <https://doi.org/10.1029/2009GB003620>
- Shiozaki, T., Kodama, T., & Furuya, K. (2014). Large-scale impact of the island mass effect through nitrogen fixation in the western South Pacific Ocean. *Geophysical Research Letters*, *41*, 2907–2913. <https://doi.org/10.1002/2014GL059835>
- Shiozaki, T., Kodama, T., Kitajima, S., Sato, M., & Furuya, K. (2013). Advective transport of diazotrophs and importance of their nitrogen fixation on new and primary production in the western Pacific warm pool. *Limnology and Oceanography*, *58*(1), 49–60. <https://doi.org/10.4319/lo.2013.58.1.0049>
- Shiozaki, T., Lee Chen, Y. L., Lin, Y. H., Taniuchi, Y., Sheu, D. S., Furuya, K., & Chen, H. Y. (2014). Seasonal variations of unicellular diazotroph groups A and B, and *Trichodesmium* in the northern South China Sea and neighboring upstream Kuroshio Current. *Continental Shelf Research*, *80*, 20–31. <https://doi.org/10.1016/j.csr.2014.02.015>
- Shiozaki, T., Takeda, S., Itoh, S., Kodama, T., Liu, X., Hashihama, F., & Furuya, K. (2015). Why is *Trichodesmium* abundant in the Kuroshio? *Biogeosciences*, *12*(23), 6931–6943. <https://doi.org/10.5194/bg-12-6931-2015>
- Taboada, F. G., Gil, R. G., Höfer, J., Gomzález, S., & Anadón, R. (2010). *Trichodesmium* spp. population structure in the eastern North Atlantic subtropical gyre. *Deep Sea Research*, *57*(2010), 65–77. <https://doi.org/10.1016/j.dsr.2009.09.005>
- Thompson, A., Carter, B. J., Turk-Kubo, K., Malfatti, F., Azam, F., & Zehr, J. P. (2014). Genetic diversity of the unicellular nitrogen-fixing cyanobacteria UCYN-A and its prymnesiophyte host. *Environmental Microbiology*, *16*(10), 3238–3249. <https://doi.org/10.1111/1462-2920.12490>
- Tripp, H. J., Bench, S. R., Turk, K. A., Foster, R. A., Desany, B. A., Niazi, F., et al. (2010). Metabolic streamlining in an open-ocean nitrogen-fixing cyanobacterium. *Nature*, *464*(7285), 90–94. <https://doi.org/10.1038/nature08786>
- Van Wambeke, F., Pfreundt, U., Barani, A., Berthelot, H., Moutin, T., Rodier, M., et al. (2016). Heterotrophic bacterial production and metabolic balance during the VAHINE mesocosm experiment in the New Caledonia lagoon. *Biogeosciences*, *13*(11), 3187–3202. <https://doi.org/10.5194/bg-13-3187-2016>
- Walsby, A. E. (1978). The properties and buoyancy-providing role of gas vacuoles in *Trichodesmium Ehrenberg*. *British Phycological Journal*, *13*(2), 103–116. <https://doi.org/10.1080/00071617800650121>
- Walsby, A. E., Kinsman, R., & George, K. I. (1992). The measurement of gas vesicle volume and buoyant density in planktonic bacteria. *Journal of Microbiological Methods*, *15*(4), 293–309. [https://doi.org/10.1016/0167-7012\(92\)90048-9](https://doi.org/10.1016/0167-7012(92)90048-9)
- Wong, G. T. F., Chung, S. W., Shiah, F. K., Chen, C. C., Wen, L. S., & Liu, K. K. (2015). Climate modulates internal wave activity in the Northern South China Sea. *Geophysical Research Letters*, *42*, 831–838. <https://doi.org/10.1002/2014GL062522>
- Wong, G. T. F., Tseng, C. M., Wen, L. S., & Chung, S. W. (2007). Nutrient dynamics and N-anomaly at the SEATS station. *Deep Sea Research*, *54*(14-15), 1528–1545. <https://doi.org/10.1016/j.dsr2.2007.05.011>
- Wu, J., Chung, S. W., Wen, L. S., Liu, K. K., Lee Chen, Y. L., Chen, H. Y., & Karl, D. M. (2003). Dissolved inorganic phosphorus, dissolved iron, and *Trichodesmium* in the oligotrophic South China Sea. *Global Biogeochemical Cycles*, *17*(1), 1008. <https://doi.org/10.1029/2002gb001924>
- Wu, K., Dai, M., Chen, J., Meng, F., Li, X., Liu, Z., et al. (2015). Dissolved organic carbon in the South China Sea and its exchange with the Western Pacific Ocean. *Deep Sea Research*, *122*, 41–51. <https://doi.org/10.1016/j.dsr2.2015.06.013>
- Xu, M. N., Zhang, W., Zhu, Y., Liu, L., Zheng, Z., Wan, X. S., et al. (2018). Enhanced ammonia oxidation caused by lateral Kuroshio intrusion in the boundary zone of the northern South China Sea. *Geophysical Research Letters*, *45*, 6585–6593. <https://doi.org/10.1029/2018GL077896>
- Yang, J. Y. T., Hsu, S. C., Dai, M., Hsiao, S. S. Y., & Kao, S. J. (2014). Isotopic composition of water-soluble nitrate in bulk atmospheric deposition at Dongsha Island: Sources and implications of external N supply to the northern South China Sea. *Biogeosciences*, *11*(7), 1833–1846. <https://doi.org/10.5194/bg-11-1833-2014>
- Zhang, Y., Zhao, Z., Sun, J., & Jiao, N. (2011). Diversity and distribution of diazotrophic communities in the South China Sea deep basin with mesoscale cyclonic eddy perturbations. *FEMS Microbiology Ecology*, *78*(3), 417–427. <https://doi.org/10.1111/j.1574-6941.2011.01174.x>